Irradiation-assisted cracking of control rod cladding

M.P.Manahan & R.Kohli
Battelle Columbus Division, Ohio, USA
J.Santucci
Electric Power Research Institute, Calif., USA
P.Sipush
Westinghouse Electric Corporation, Pa., USA
R.L.Harris
Wisconsin Electric Power, USA

ABSTRACT

Severe wear and cracking have been observed in the cladding of rod cluster control assemblies (RCCAs) at various pressurized water reactors (PWRs) in the United States. The cracks are typically about 4 inches long, oriented longitudinally, and located in the high-fluence region of the rods. This paper reports our findings concerning the cause and nature of the cracking mechanism. Data from miniature-specimen tensile tests, scanning electron microscopy (SEM) investigations, and corrosion tests on control rod cladding that failed in service are reported along with a discussion of the microstructural evolution and the possible causes for failure.

1 INTRODUCTION

A study was initiated by the Electric Power Research Institute (EPRI) to develop new operating guidelines and inspection methods to help utilities predict and extend the service life of PWR control rods. The specific objectives of this program were: to correlate actual wear data on the RCCA rods with wear estimates from site photographs; to determine the cause of cladding cracking; and to estimate the performance of RCCAs while taking into consideration cladding wear and cracking. This paper reports primarily on our findings regarding the in-service cracking mechanism. Details of the overall test program were reported by Sipush et al. (1986).

The mechanism of irradiation-assisted stress-corrosion cracking (IASCC) has been suggested as a possible explanation for the observed failures. Recent constant extension rate tests by Clarke and Jacobs (1983) on annealed Type 304 stainless steel (SS) revealed a fluence effect on intergranular stress-corrosion cracking (IGSCC) resistance. Samples irradiated to a fast-neutron fluence of 3.0×10^{21} n/cm^2 were observed to fail entirely by IGSCC when tested in 288 C water containing 32 to 36 mg/l of dissolved oxygen. Another specimen irradiated to 1.0×10^{18} n/cm^2 was tested under identical conditions and failed in a ductile mode. Thus, there appears to be an incubation dose above which the microstructure evolves to a state that promotes IGSCC.

In the present study, miniature specimen tensile tests, SEM investigations, and corrosion tests were performed on samples

Table 1. Postirradiation tensile properties of irradiated Type 304 SS 10 percent cold-worked tubing determined using miniature specimens (Manahan and Kohli 1985).*

Speci-men No.	Strain Rate (sec^{-1})	IG Fracture (%)	Yield Stress (0.2% offset) (MPa)	Ultimate Tensile Stress (MPa)	Fracture Stress (MPa)	Uniform Strain (%)	Fracture Strain (%)
C-1	5.0×10^{-4}	0	909	924	703	3.3	8.0
C-2	1.0×10^{-6}	3-4	936	944	708	1.6	9.3
C-3	2.0×10^{-7}	15-20	**	865	809	**	4.3
C-4	1.0×10^{-8}	30-35	**	848	577	2.6	6.8
D-1	1.0×10^{-6}	6	763	792	577	2.7	15.0

* The test temperature was 315 C and the atmosphere was argon gas for all tests reported here.

** These data cannot be reported due to uncertainty in the load-time record.

obtained from a PWR (Point Beach Unit 1) irradiated RCCA that failed in service. The irradiated material was sectioned into four tube segments approximately 2.5 cm long. The tube identifications used are C (5.0×10^{21} n/cm^2), D (4.0×10^{21} n/cm^2), E (2.0×10^{21} n/cm^2), and F ($\sim$ 0 fluence) in order of decreasing fluence.

2 MINIATURE-SPECIMEN TESTS

Important constraints in selecting an appropriate test method were the limited amount of material available and the steep axial fluence gradient along the length of the control rod from which specimens could be obtained. Also, it was not desirable to perform tensile tests on the entire tube sections since this would severely limit the amount of data obtainable per unit volume. To satisfy these constraints, we used the patented Battelle miniature slow strain rate tensile behavior test (Manahan et al. 1986). It is possible to obtain 10 miniature tensile specimens from a tube length of 23.0 mm that will yield data approximately equal in accuracy to conventionally tested tube specimens.

To demonstrate the accuracy and validity of the miniature tensile specimens, three such specimens were prepared from prototypic, unirradiated Type 304 SS tubing and then tested. The miniature-specimen results were compared with the results of uniaxial tensile tests on three tubes from the same lot of material. The miniature-specimen tests were performed at room temperature and at a strain rate of 5.0×10^{-4}/sec. The miniature-specimen data were reproducible and compared well with the large-specimen data.

The main purpose of the postirradiation tensile tests was to determine whether the IG cracking mode observed in-reactor could occur in an inert atmosphere. The results of these tests are given in Table 1.

The first test (specimen C-1) was performed at a strain rate of 5.0×10^{-4}/sec as a reference to provide a comparison with the unirradiated tensile properties of the material. A significant increase in the yield strength from 496 to 909 MPa was measured. As expected, no IG fracture was observed due to the high strain rate. The next two tests (C-2 and D-1) were performed at a slow strain rate of 1.0×10^{-6}/sec. In these tests, IG cracking was observed over a small percentage of the fracture surface. The effect of fluence and strain rate on the tensile behavior was evident. The next test (C-3) was run at a strain rate of 2.0×10^{-7}/sec, which produced considerably more IG fracture; the fracture strain also was less than in the previous tests. For specimen C-4, the strain rate was decreased to 1.0×10^{-8}/sec and considerably more IG fracture was observed. The IG cracking always appeared on the inner-diameter surface of the specimen and started at about the same location. These data demonstrate that it is possible to obtain IG fracture in an inert environment above a threshold fluence. Also, the data further confirm that the amount of IG fracture is dependent on the strain rate for a given fluence.

3 MICROSCOPY AND CORROSION TESTING

3.1 Scanning Electron Microscopy

The fracture surfaces of the five tensile specimens, C-1, C-2, C-3, C-4, and D-1, were examined with an ISI Model Super II scanning electron microscope equipped with a Tracor Northern energy-dispersive analyzer. Except for specimen C-1, which showed only the characteristic dimples typical of ductile fracture, the fracture surface of the other specimens revealed regions of brittle failure within a predominantly ductile fracture surface. The amount of brittle fracture was dependent on the strain rate, ranging from approximately 3 percent of the total fracture area for specimen C-2 to 30-35 percent of the total fracture area for specimen C-4. Brittle fracture generally initiated intergranularly near one end of the specimen, although multiple regions of IG crack initiation were often observed on the inside diameter of the specimens.

Careful examination of the fracture surface revealed the presence of several particles containing sulfur, silicon, aluminum, nickel, and zinc in the grain boundaries. Radiation-enhanced diffusion may be responsible for the transport of these species to the boundaries (Jones 1985). Also, zinc is known to embrittle stainless steel by the liquid metal embrittlement mechanism (Old 1980), whereas sulfur is known to promote stress-corrosion cracking (Berry 1971). The presence of aluminum and nickel suggests the possible formation of a Ni_3Al high-strength, low-ductility intermetallic compound. The presence of these elements in the particles at the grain boundaries and the existence of an IG fracture region suggest that more than one failure mechanism could be operating in these specimens.

3.2 Corrosion Testing and Metallographic Examination

A nitric acid-potassium dichromate corrosion test was performed on specimens C-2, D-1, E-3, and F-3 to determine the extent of IG penetration. Following corrosion testing, the specimens were examined metallographically at high magnification and the average depth of IG penetration was determined from a large number of individual measurements.

The weight-change data for each specimen following 4-, 8- and 12-hour exposure times are given in Table 2, which also lists the average depth of penetration. These results suggest a small but distinct fluence dependence on the extent of IG penetration of the specimens.

4 IN-SERVICE CRACKING MECHANISM

Instances of hairline cladding cracks have been observed during site inspections of RCCAs. At the Point Beach PWR, two cracked rodlets were found after 11 cycles of operation. The observed cracks are located near the rodlet tips and are approximately 4 to 6 inches long.

Based on the data obtained from the hot cell program (Sipush et al. 1986) on one cracked rodlet tip and one reference intact rodlet tip, it appears that the cracking mechanism is related to stresses produced by absorber/cladding mechanical interaction and to irradiation damage of the cladding. The most probable effect of irradiation is radiation-enhanced segregation of the impurity elements to the grain boundaries (Jones 1985, Brimahll et al. 1984). It has been shown from in-pile data that cladding materials with reduced silicon and phosphorus are less prone to cracking (Garzarolli et al. 1985).

Based on the results of the miniature tensile tests of irradiated cladding material in an inert environment, it appears that irradiation alone could be sufficient to render the cladding susceptible to IG cracking. Figure 1 shows the percent IG fracture of irradiated cladding in an inert atmosphere as a function of strain rate. Autoclave tests representative of a typical PWR coolant would have to be performed at low strain rates to determine the relative contribution of the environment to the in-pile cracking. Such tests could determine the extent to which stress corrosion plays a role in the in-pile cracking mechanism.

The source of the stress that causes cracking in RCCA rodlets is absorber contact with the cladding. The magnitude depends on a combination of the following: possible plastic deformation (yielding) of the absorber material due to axial forces during power stepping in service; tolerances; and wall thinning of the cladding due to wear caused by contact of the cladding with the fuel assembly guide thimble at the rodlet tip. Absorber swelling, plastic deformation, and relative thermal expansion would contribute to absorber/cladding gap closure during service and tolerances would affect the initial gap. Wall thinning would cause an increase in the local hoop stress in the thinned area. One of the most significant differences between the cracked tip and the reference tip was the observed wall thinning in the cracked rodlet. The crack occurred in the thinned area.

Table 2. Results of corrosion testing (Manahan and Kohli 1985).

Specimen Number	Weight Loss (mg/cm^2) After 4 hr	8 hr	12 hr	Average Depth of Penetration (μm)
C-2	4.43	21.30	60.75	45.97
D-1	+3.55*	14.18	56.74	40.89
E-3	9.51	25.35	63.38	37.85
F-3	3.54	14.15	14.15	37.08

* After 4 hours specimen D-1 exhibited a net weight gain of 3.55 mg/cm^2 which may be due to an atypical incubation period (Jacobs and Dunning 1983) in this specimen.

The metallography of the cracked tip showed 100-percent IG fracture and no necking or ductile lip. The profilometry showed no plastic deformation of the cladding. These results, which indicate that the cracking occurred below the yield stress, are consistent with the tensile test results.

The cracking mechanisms appear to be generic; that is, cracking can occur in Type 304 SS cladding irradiated to high fluences, at stresses below the general yield stress, as a result of mechanical interaction between the absorber and the cladding. However, more data are needed to better quantify the influence of variables such as fluence, manufacturing tolerances, and number of power-stepping events on the cracking frequency. Based on the number of cracked rodlets observed to date in operating RCCAs, it would appear that the incidence of cracking is small below about nine cycles of reactor operation.

There is no apparent impact of these cracks on the performance or service life of RCCAs since no evidence exists that longitudinal hairline cracks affect the functional requirements of an RCCA. The rodlets do not become distorted as a result of the cracks and no increase in diameter was observed. The cracks are longitudinal, and although branching cracks are seen, they are unlikely to lead to separation of the component parts or to affect axial design stresses. The amount of absorber corrosion that occurred in the cracked rodlet due to coolant entering through the crack did not result in any degradation that would affect the functional requirements of an RCCA.

5 COMPARISON WITH LITERATURE DATA

The IASCC of Type 304 SS has been the subject of research by several investigators. Austenitic alloys exposed to high neutron fluences and radiolytic oxidizing radicals have failed intergranularly under tensile stress fields. In-reactor failure of Type 304 SS, 304L SS, 347 SS and 348 SS, Inconel 800 and 625, and other alloys has been observed for boiling water reactor (BWR) and PWR fuel rods, BWR control blade rodlets, sheaths, and handles, neutron source holders, source range monitors, intermediate range monitors, and test capsules (Jacobs 1986). The cracking observed in the Point Beach PWR control rods may be another example of the same failure mechanism.

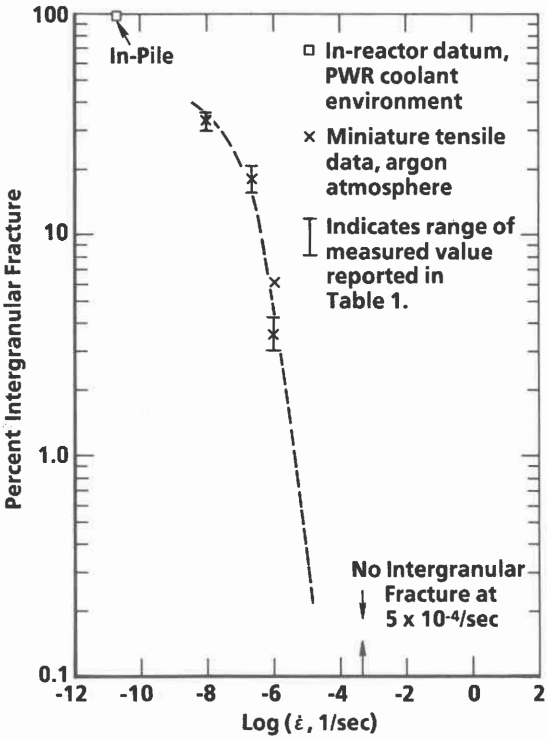

Figure 1. Percent intergranular fracture versus strain rate for irradiated cladding tensile tests at 315 C. Figure from Sipush et al. (1986), data from Manahan and Kohli (1985).

Armijo (1967) and Aust (1969) theorized that impurity segregation to the grain boundaries of austenitic alloys provides a continuous path for corrosion attack in the absence of a continuous carbide network (for example, nonsensitized, solution-annealed material). Duncan (1968) reported evidence in support of these theories. Duncan found that carbon, silicon, and phosphorus at grain boundaries increased both IGSCC and IGSCC susceptibility of nonsensitized austenitics. Furthermore, irradiation was found to increase susceptibility in PWR and BWR SS fuel cladding samples irradiated to burnups of up to 35 MWd/kgU. In Duncan's work, the failure of cold-worked and annealed SS fuel rod cladding in the Vallecitos BWR and the Connecticut Yankee PWR were attributed to IASCC, where the applied tensile stresses resulted from pellet-cladding mechanical interaction. High-purity SS was found to be more resistant to IGSCC both in the laboratory and during reactor service. Two alternate screening methods were developed to identify susceptible materials prior to irradiation: exposure to a boiling solution of nitric acid-dichromate and exposure to a ferric chloride solution at 343 C. These methods provided consistent results that could be related to the in-reactor performance data. Figures 2 and 3 show a comparison

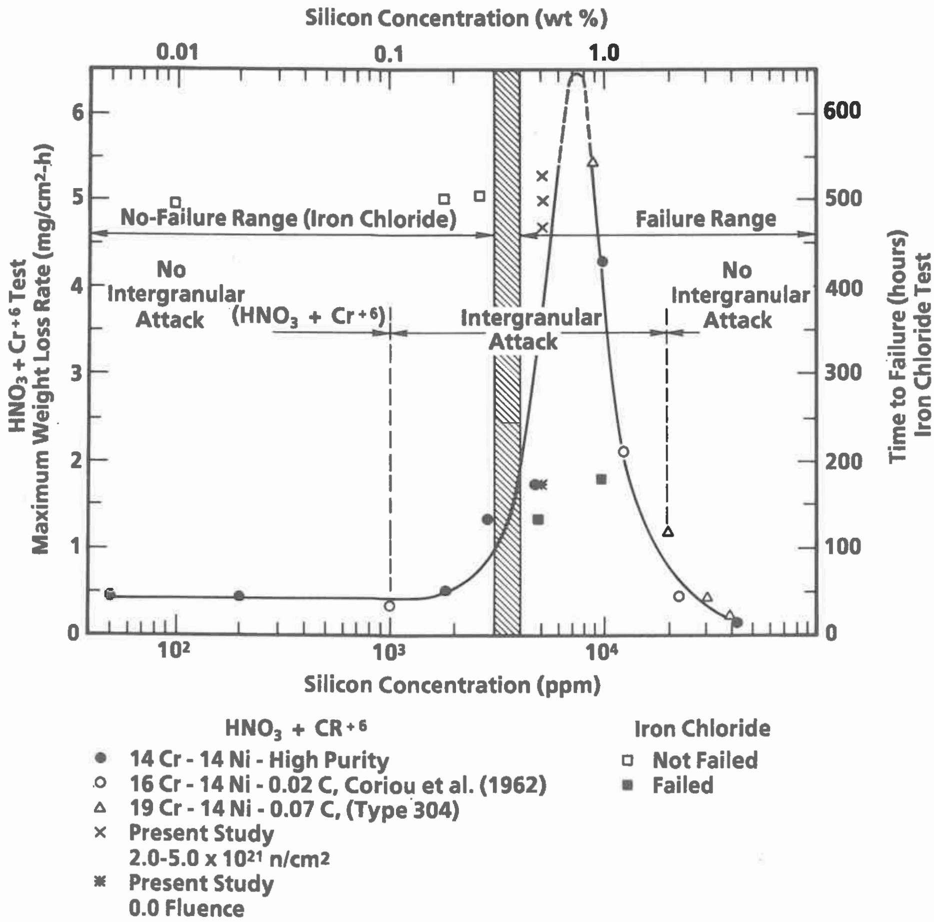

Figure 2. Effect of silicon additions on the corrosion resistance of nonsensitized, high-purity SS alloys. Figure from Duncan (1968) with data from present study added.

of Duncan's data with those from the present study. The test conditions for both experiments were similar and the silicon and phosphorus concentrations for the Point Beach specimens were assumed to be the nominal values for this class of steel. This comparison shows consistency of results, indicating that the material used for the Point Beach PWR control rods is susceptible to IASCC and that the susceptibility increases with exposure, as was found by Duncan.

In an EPRI research program, Garzarolli and Stehle (1986) tested several austenitic alloys under controlled strain rate conditions in both BWRs and PWRs. The results of these tests (Figure 4) indicate a parabolic dependence of strain-to-failure on irradiation fluence. At fluences greater than about 6.0 x 10^{21}n/cm^2, materials that are susceptible to radiation-enhanced impurity segregation (to grain boundaries), and to IG corrosion cracking, fail at essentially 0-percent strain. These results are consistent with those observed on the Point Beach PWR components examined in the present study.

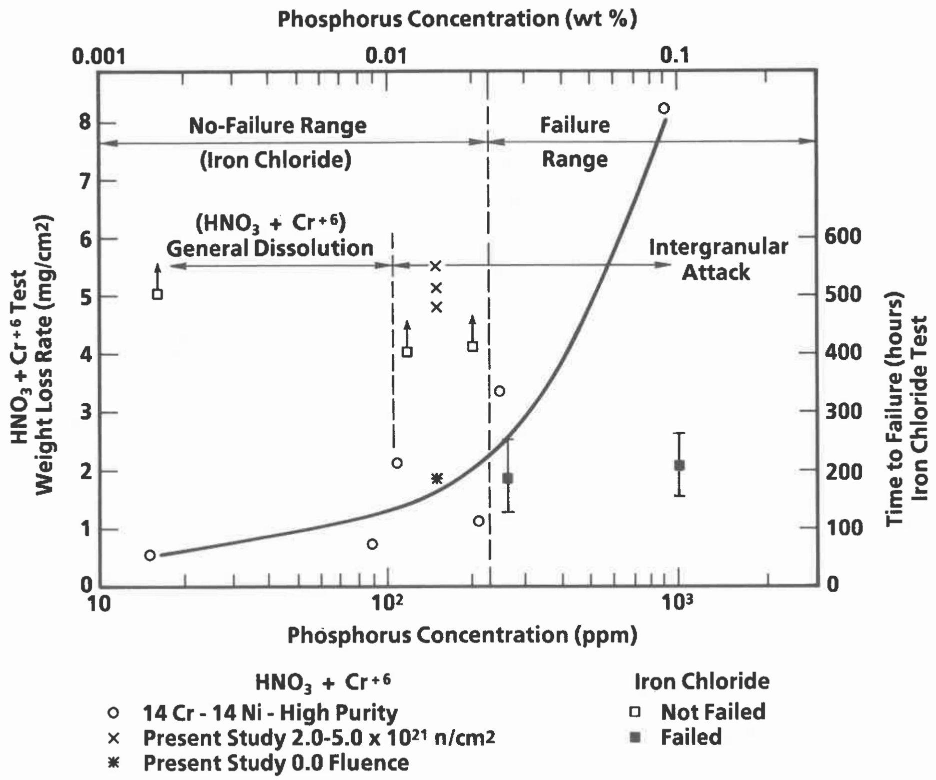

Figure 3. Effect of phosphorus additions on the corrosion resistance of nonsensitized, high-purity SS alloys. Figure from Duncan (1968) with data from present study added.

Garzarolli also has found that high-purity (low phosphorus and silicon) Type 348 SS has superior resistance to in-reactor IASCC.

6 SUMMARY AND CONCLUSIONS

A fast-neutron incubation fluence is necessary to change the material microstructure such that IG cracking is possible in Type 304 SS. IG fracture may occur in an inert environment in Type 304 SS provided that the material has been irradiated past the incubation dose and the strain rate is sufficiently low ($\sim 10^{-6}$/sec). It is likely that IG failure will be more widespread in irradiated stainless steel tested in a corrosive environment, but additional work is necessary to confirm this.

Particles containing sulfur, silicon, aluminum, nickel, and zinc were discovered in the grain boundaries of the highly irradiated Type 304 SS. Radiation-enhanced diffusion may be responsible for the transport of these elements to the grain boundaries. The presence of these elements and the existence of an IG fracture region suggests

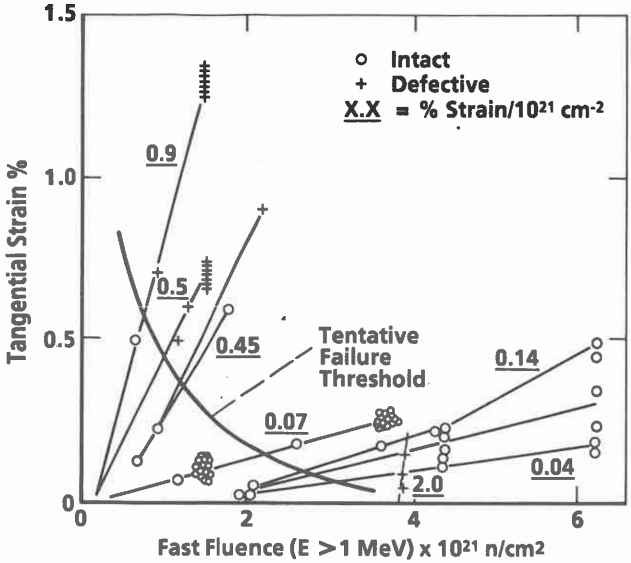

Figure 4. Map of experience with austenitic SS strained in the core of PWRs. Figure from Garzarolli and Stehle (1986).

that more than one fracture mechanism could be operating in this irradiated material.

Instances of IASCC in Type 304 SS and other austenitic alloys have been reported and analyzed for cases where the environment is highly oxidizing (BWR), and this cracking was found to occur in susceptible materials under conditions of very low stress. IASCC also has been studied in less oxidizing environments (PWRs). At high exposures, susceptible materials have failed at relatively high applied loads. The data from Garzarolli and Duncan provide evidence of this, as do the results of investigations on the causes of fuel failure in 20-percent cold-worked Type 304 SS clad fuel rods in the Connecticut Yankee PWR (EPRI 1981, 1982). The data from the Point Beach PWR components suggest that irradiation-assisted IG cracking of commercial-purity Type 304 SS can occur in PWR environments at very high exposures and under conditions of very low applied stresses. An important but as yet unresolved issue is the identification of the active corrodent in the PWR environment. In particular, it is not clear whether sufficient radiolytic oxidizing radicals exist in the PWR environment to promote such failures, or whether other species in the coolant, such as LiOH, play an active role.

ACKNOWLEDGEMENT

This work was performed under contract to EPRI, research project number 1628-4.

REFERENCES

Armijo, J.S. 1967. Impurity absorption and intergranular corrosion of austenitic stainless steel in boiling $HNO_3K_2Cr_2O_7$ solutions. Corr. Sci. 7:143.

Aust, K. T. et al. 1967. Heat treatment and corrosion resistance of austenitic Type 304 stainless steel. Trans. ASM. 59:544.

Berry, W. E. 1971. Corrosion in nuclear applications. New York: Wiley.

Brimahll, J. L., D. R. Baer & R. H. Jones. 1984. Radiation-induced phosphorus segregation in austenitic and ferritic alloys. J. Nucl. Mater. 122 & 123:196-200.

Clarke, W. L. & A. J. Jacobs. 1983. Effect of radiation environment on SCC of austenitic materials. Proc. of the first international symposium on environmental degradation of materials in nuclear power systems--water reactors, August 22-25.

Coriou, H. et al. 1962. Comptes Rendus. 254:4467.

Duncan, D. R. 1968. Stainless steel failure investigation program final summary report; joint US-Euratom research and development program. EURAEC/GEAP-5530.

EPRI 1981. Investigation of stainless steel clad fuel failures and fuel performance in the Connecticut Yankee reactor. EPRI NP-2119.

EPRI 1982. Evaluation of stainless steel cladding in PWRs. EPRI NP-2642

Garzarolli, F. et al. 1985. Deformability of Austenitic Stainless and Ni-Base Alloys in the Core of a Boiling and a Pressurized Water Reactor. Proc. of the second international symposium on environmental degradation of materials in nuclear power systems--water reactors, September 9-12.

Garzarolli, E. F. & H. Stehle. 1986. Behavior of structural materials in LWR power reactors. Inter. Symp. on improvements in water reactor fuel technology and utilization, September 15-19. IAEA-SM-288/24.

Jacobs, A. J. & G. E. Dunning. 1983. Correlation of weight and tensile strength loss with depth of intergranular attack in the HNO_3/Cr^{+6} corrosion test. Report no. A00-483, General Electric Company.

Jacobs, A. J. 1986. Effects of impurities and grain size on irradiation-assisted IGSCC of Type 304 SS and 348 SS. EPRI RP 2058-8

Jones, R. H. 1985. Some radiation damage-stress corrosion synergisms in austenitic stainless steel. Proc. of the second intl. symp. on environmental degradation of materials in nuclear power systems--water reactors, September 9-12.

Manahan, M. P. & R. Kohli. 1985. Examination and testing of irradiated control rod tubing. Final report to Westinghouse Electric Corp. Battelle Columbus Division.

Manahan, M. P., A. S. Argon & O. K. Harling. 1986. Determining mechanical behavior of solid materials using miniature specimens. U.S. patent number 4,567,744.

Old, C. F., 1980. J. Nucl. Mater. 91:2.

Sipush, P. J., J. Woodcock & R. W. Cherkering. 1986. Lifetime of PWR silver-indium-cadmium control rods. EPRI-NP-4512.